PERGAMON

International Journal of Multiphase Flow 27 (2001) 797–816

International Journal of Multiphase Flow

www.elsevier.com/locate/ijmulflow

Effect of tube diameter on flooding

M. Vijayan, S. Jayanti *, A.R. Balakrishnan

Department of Chemical Engineering, Indian Institute of Technology, Chennai 600 036, India

Received 8 February 2000; received in revised form 30 July 2000

Abstract

This paper describes an experimental study on the effect of tube diameter on the mechanism of flooding in vertical gas–liquid countercurrent annular flow. Flooding experiments were conducted with three different tube inner diameters, namely, 25, 67 and 99 mm with smooth inlet and outlet conditions for air and water. The results indicate that the mechanism of flooding is qualitatively different in the small and the large diameter test sections. While flooding in the 25 mm diameter section occurred essentially by the upward movement of large waves created near the liquid outlet, no such waves could be seen in the 67 and the 99 mm diameter test sections. Here, flooding occurred by droplet carryover or by an unstable, churn-like motion in the liquid film. The results are compared with existing correlations. The effect of test section length on flooding was also investigated.

1. Introduction

Flooding is closely associated with the limit of stable countercurrent gas–liquid flow and as such it is an important design criterion in a variety of process equipment such as falling film absorbers, evaporators, heat pipes, reflux condensers and in some aspects of nuclear reactor safety. Although flooding has been studied for a number of decades, there is still some uncertainty about the precise mechanism by which flooding takes place in countercurrent gas–liquid annular flow. It is generally believed (Suzuki and Ueda, 1977; McQuillan et al., 1985; Govan et al., 1991) that flooding occurs when large waves, formed near the liquid outlet, are swept upwards by the gas phase. However, recent experiments involving careful measurements of the film thickness (Zabaras and Dukler, 1988; Biage, 1989) did not reveal the presence of these upward-moving waves at the flooding point. In some cases, this discrepancy can be attributed to the inlet and outlet conditions for the gas and liquid phases (Govan et al., 1991), however, the experiments of

* Corresponding author. Tel.: +91-44-4458227; fax: +91-44-2350509.
E-mail address: sjayanti@iitm.ac.in (S. Jayanti).

0301-9322/01/$ - see front matter
PII: S0301-9322(00)00045-8

Biage (1989) showed that even with smooth inlet and outlet conditions for both phases, sustained upward-moving waves were not observed. In a recent theoretical study, Jayanti et al. (1996) adduced the tube diameter as the determining factor in the way that flooding occurs. They argued that flooding could occur by one of two mechanisms, namely, upward transport of waves created near the liquid outlet and carryover of droplets created in the test section. If a large roll wave was formed in a test section, then it would experience greater drag force in a small diameter test section than in a large diameter test section. Thus, the roll waves which are formed on a falling film would be more likely to be swept upwards in a small diameter tube. Using estimates of the drag force on waves, they argued that the gas flow rate required to drag a wave upwards in a large diameter tube would be higher than that required to initiate flooding by the droplet entrainment mechanism in the same tube at the same liquid flow rate. This would explain the absence of upward-moving waves in the experiments of Zabaras and Dukler (1988), who used a test section diameter of 50.8 mm. All the experiments in which upward-moving waves were reported had tube diameters of less than 32 mm.

The mechanism proposed by Jayanti et al. (1996) appears plausible but it is based, not on experimental observations, but on estimates of drag forces on assumed wave shapes on a falling film. The limitations of their calculations and estimates can be gauged from the fact that their model fails to reproduce the well-established effect of increasing liquid flow rate on the flooding gas velocity. In spite of this, it is felt that there is a case for investigating systematically the effect of tube diameter on flooding. To this end, countercurrent flow experiments have been conducted in test sections of 25, 67 and 99 mm tube diameters wherein the mechanism of flooding was observed visually. The results indicate that there is indeed a strong effect of tube diameter on flooding, but in a way that was not foreseen by Jayanti et al. (1996) in their theoretical study.

2. Experimental details

2.1. Flow circuit

The experimental setup used in the present study is shown schematically in Fig. 1. It consists of three countercurrent flow columns having internal diameters of 25, 67 and 99 mm with common air and water connections. Air is fed to the test section from one of the three air compressors (with maximum capacities of 8, 20, and 200 m^3/h at STP conditions) connected in series. A needle valve, located just before the entrance to each test section, is used for flow control. Water is pumped from a reservoir through a pre-filter and is fed into the test section by two pumps, each having a capacity of 0.5 hp, connected in series. A bypass circuit is provided to minimize the load on the pumps and to control the water flow rate under low flow rate conditions.

Each column is made of transparent acrylic plastic material and has a total length of 4 m. Water enters and exits from the test section through a filter assembly to provide smooth inlet and outlet conditions. The filter assembly consists of three elements: a thin stainless mesh which provides large resistance to flow; a perforated cylindrical plate, which provides rigidity to the mesh; and an outer cylinder which houses the two and which is connected to the pump or the reservoir through a valve. The stainless steel mesh consists of three layers. The inner layer has a nominal pore size of 25 μm and is enclosed in two layers of nominal pore size of 100 μm. This

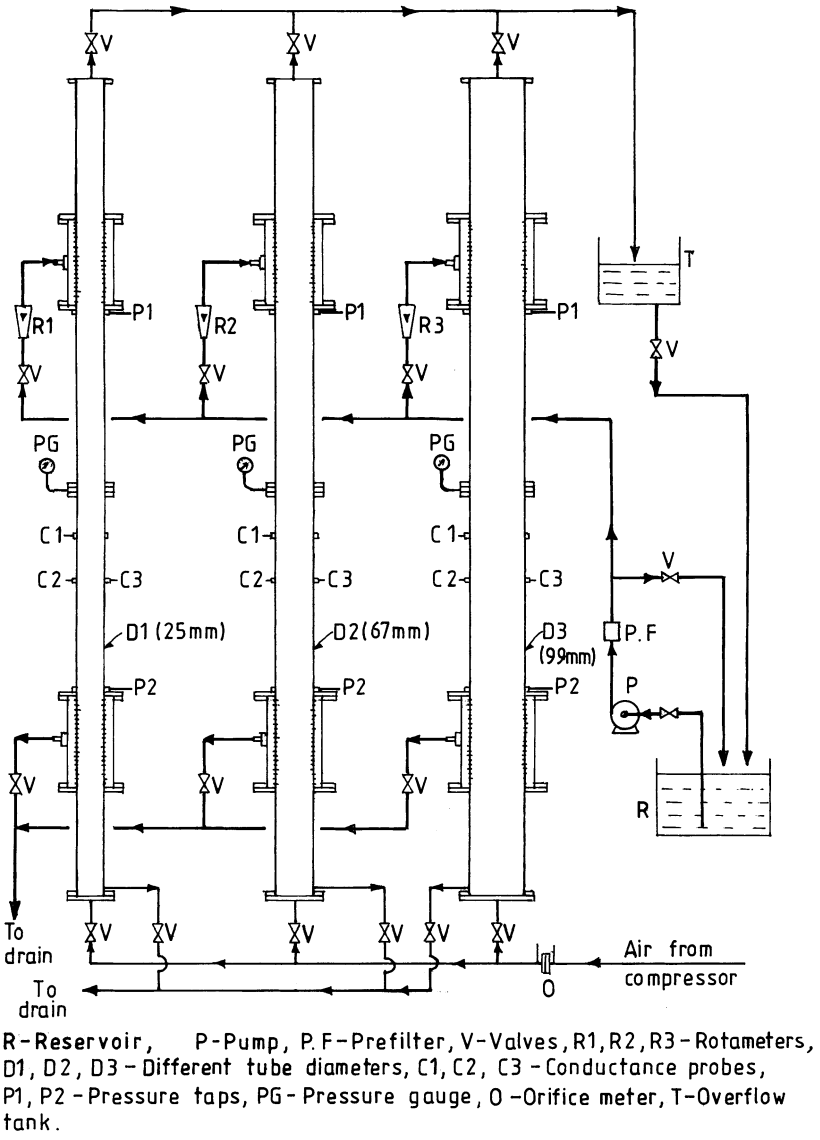

Fig. 1. Schematic diagram of the ring assembly showing the three test sections.

mesh is wrapped tightly and tack-welded on to the *inside* of a cylindrical perforated plate having an inner diameter slightly greater than that of the test section such that the whole assembly has an inner diameter equal to that of the test section. The perforated cylinder is fixed inside a perspex cylinder with three nozzles to which flexible hoses are connected to feed water into the test section in the case of an inlet and to remove water from it in the case of an outlet. In this filter assembly, the cylindrical perforated plate provides the rigidity to withstand the large pressure drop across the mesh to maintain uniform flow while the three sheets of stainless mesh prevent jet formation and ensure smooth and uniform entry around the circumference of the test section. The inner and

the outer cylinders are fixed rigidly between two flanges, and this whole assembly is connected to the test section to serve as inlet/outlet for the water.

The height of each column was 4 m; however, the length of test section, i.e., the height between the water inlet and the water outlet, was 2.0 m for the 25 mm diameter test section and 1.8 m for the 67 and 99 mm diameter test sections. There is thus about 1 m length of pipe each below and above the test section, which serves to provide smooth inlet and outlet conditions for the air flow as well. Air and water, if any, leave the test section from the top through a PVC pipe and are separated in an open tank. Water is fed back to the main water tank by gravity. The pressure in each column could be controlled by a valve located in the PVC pipe.

2.2. Setup for flow visualization studies

One of the aims of the experiments was to observe visually the nature of the interface structure, e.g., presence of upward/downward moving large waves, droplet formation, etc., in countercurrent flow. This was done by the naked eye initially, but still photography and videography were used to help visualize the flow structure. In still photography, the camera was fixed on a stand very close to the visualization section and the flash was fixed at an angle of 180° to the camera. The flash was electronically connected to the camera so that the camera shutter could open at the same time as the flash. After preliminary experiments, it was decided that good pictures could be obtained with a flash duration of 1/30,000th of a second. Video pictures, at a speed of 30 frames per second, were taken of the entire column to obtain a better understanding of the relation, if any, between events happening at the outlet and those at the inlet.

2.3. Instrumentation

The primary variables that were measured during the experiments were the pressure, the pressure drop, the input flow rate of each phase, the flow rate of water, if any, through the water outlet and the film thickness. Air and water flow rates into the test section were measured using an orifice meter and a bank of rotameters, respectively. The static pressure in the column was measured using a pressure guage, while the pressure drop was measured using water or mercury-filled manometers. The water flow rate through the top outlet, if any, was determined by collecting it in a measuring flask over a period of time. The temporal variation of the film thickness was measured using two-pin type of conductance probes (Hewitt, 1982; Jayanti et al., 1990), but these are not discussed in the present paper.

2.4. Experimental procedure

The above setup has been used to measure pressure drop and film thickness for a range of air and water flow rates through a given test section. In each run, the water flow rate was set at a specified level, and the air flow rate was increased in small increments from a pure falling film case. After each increment in the air flow rate, the flow was allowed to settle for a few minutes and the flow rate of each phase, the pressure drop in the test section and the film thickness at three locations in the test section were recorded. The flow structure, e.g., presence of large waves, droplets, etc., was observed by the naked eye and recorded. (High speed photography and

videography of the flow were done separately.) The water flow rate through the top outlet, if any, was collected in a measuring flask over a period of time. After these measurements were over, the air flow rate was further increased by a small increment. These measurements and observations were made at several air flow rates right up to and beyond the point of flooding. The experiments were *not* conducted at constant inlet pressure condition, and the test section pressure was allowed to change from run to run although the variation was small. The maximum test section pressure at the highest air flow rates for each water flow rate was typically of the order of 0.5 bar (gauge). The results from several such experimental runs, conducted in three diameter columns over a range of water flow rates, are discussed below.

3. Mechanism of flooding

3.1. Criterion for flooding

It is generally agreed that flooding marks the limit of stable countercurrent flow. Any further increase in either the gas flow rate or the liquid flow rate would destabilize the countercurrent flow to form co-current flow above the liquid inlet. The instability of countercurrent flow is manifested in several ways (Bankoff and Lee, 1982):

(i) sudden rise in the pressure gradient in the test section,
(ii) appearance of a sustained liquid flow above the liquid inlet,
(iii) reduction in the down flow rate of the liquid,
(iv) appearance of a highly disturbed film flow.

All these effects are inter-related. For example, the highly disturbed film flow results in a large increase in the pressure gradient and a reduction in the down flow rate can be sustained only if the rest of the input liquid is carried away by the gas stream beyond the liquid inlet. In addition to this, it is sometimes claimed (Clift et al., 1966; Zabaras and Dukler, 1988) that the down flow rate in the post-flooding regime is constant and that the liquid down flow rate at the flooding point is the maximum possible down flow rate for a given gas flow rate. Any of these effects can be, and have been, used as a criterion to detect the onset of flooding in countercurrent flow. As a modification to (ii) above, Govan et al. (1991) defined flooding as the point at which liquid appeared (and not necessarily carried away by the gas stream) above the liquid injection point. In addition to these, the way flooding is induced may also give rise to potentially conflicting results. For example, McQuillan et al. (1985) and Govan et al. (1991), among others, used slight depressurization, of the order of 0.05 bar, to induce flooding while others such as Dukler and Smith (1982) and Zabaras and Dukler (1988) induced flooding by gradually increasing the air flow rate. In view of the possible discrepancies that may arise in using these various criteria to determine the flooding point, careful experiments have been performed to identify the phenomena that occur in gas–liquid countercurrent flow. These are discussed below.

3.2. Phenomena in countercurrent flow

The various phenomena that occur in countercurrent flow are best understood by studying the flow parameters as the air flow rate is increased in small steps while maintaining a constant inlet

liquid flow rate. A typical set of results obtained in one such run in the 25 mm diameter tube is shown in Fig. 2. Here, the water flow rate was set at 0.0278 kg/s and the air flow rate was varied over a wide range. The pressure gradient and the down flow rate of water are plotted as a function of the air flow rate. Several still photographs of the test section were also taken with a flash duration of 1/30,000th of a second, and some of these are shown in Fig. 3 to illustrate the interface structure. Interfacial waves are present even when there is no air flow rate (Fig. 3(a)). However, these appear to be of fairly small amplitude. The corresponding point in Fig. 2 is marked as point A and it can be seen that the pressure gradient is very small. As the air flow rate is increased, larger amplitude waves begin to form and occasionally droplets are sheared away from it. This phenomenon is captured on camera and is shown in Fig. 3(b). This point is marked B on the pressure gradient plot (Fig. 2) and it can be seen that the pressure gradient under these conditions (of onset of droplet entrainment) is still very small. At slightly higher air flow rates, the rate of entrainment of droplets increases and more drops can be seen in the tube (Fig. 3(c)). However, these are confined to the bottom half of the test section and no droplets are carried beyond the liquid inlet. At this point, large waves are formed occasionally but the pressure gradient remains very small. As the air flow rate is further increased, the distortion of the interface becomes more pronounced (Fig. 3(d)) and the wave amplitude appears to increase tremendously. However, the waves are not coherent circumferentially. The pressure drop at this point, marked D in Fig. 2, is higher than at point A but is still considerably less than that at flooding. Just before flooding (Fig. 3(e)), large amplitude, ring-type waves are formed and the interface becomes highly dimpled. One notable feature is the absence of droplets; in the 25 mm diameter tube, the droplet

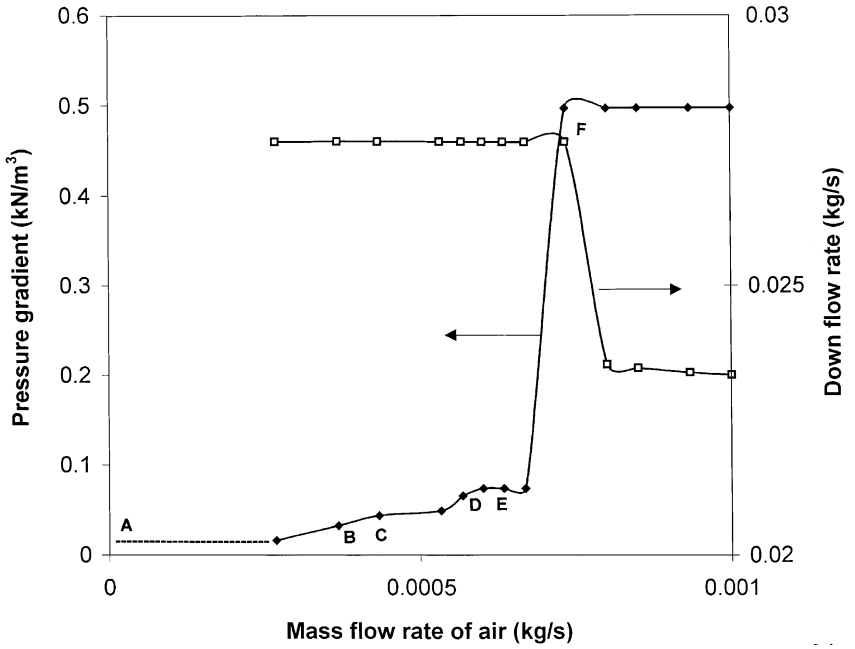

Fig. 2. Variation of the pressure gradient and the down flow rate with air flow rate at a water flow rate of 0.0278 kg/s in the 25 mm diameter section.

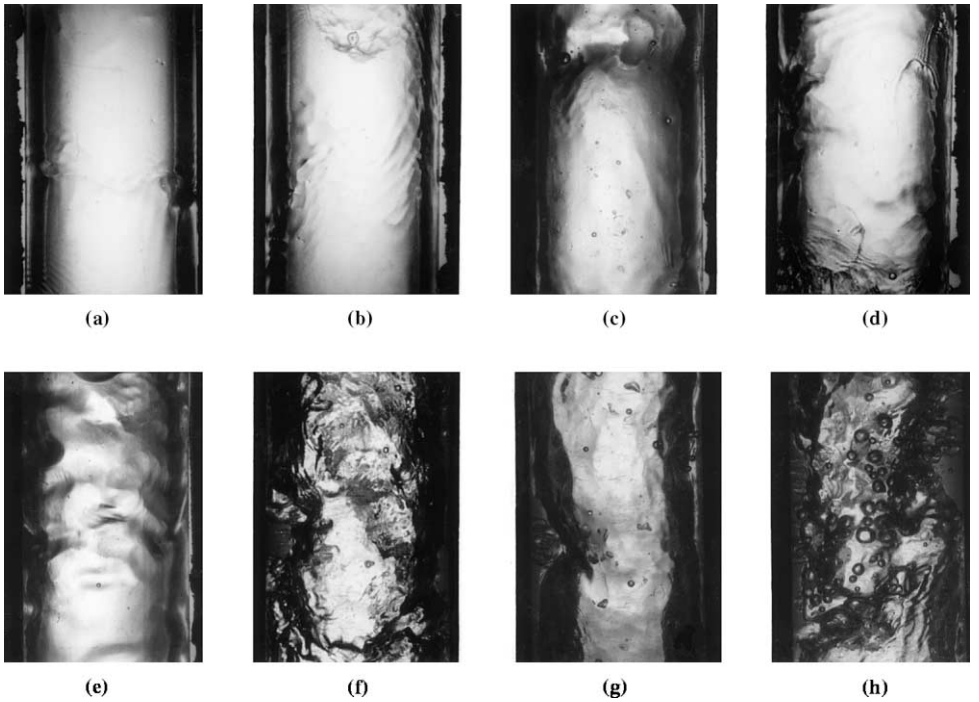

Fig. 3. Still photograph of the flow in the 25 mm diameter test section at a water flow of 0.0278 kg/s and at an air flow rate of: (a) 0; (b) 0.0036; (c) 0.000433; (d) 0.00060; (e) 0.00066; (f) 0.00085; (g) 0.00133; (h) 0.0037 kg/s.

concentration remains very small right up to flooding. The pressure drop still remains low (point E in Fig. 2). At flooding point, some of these large amplitude waves are carried up repeatedly and fairly periodically. The structure of the interface within this upward-moving wave appears to be chaotic with large amplitude waves (Fig. 3(f)) being present on the interface. The pressure drop becomes very high (point F in Fig. 2). The flow structure in post-flooding conditions is typically characterized by considerable entrainment of bubbles in the liquid film (Figs. 3(g) and (h)). Fig. 2 indicates that the pressure gradient remains very high although this is not higher than the value at point F.

Fig. 4 shows several still photographs taken in the 67 mm diameter tube near the liquid outlet for a water flow rate of 0.111 kg/s. In Fig. 4(a), where there is no air flow, the interface appears to be covered with a number of waves and the interface appears rougher than the corresponding one in the 25 mm diameter test section (Fig. 3(a)). As the air flow rate is increased, larger amplitude waves are formed from which droplets are torn off. This results in the formation of number of droplets at various sizes (Figs. 4(b) and (c)) unlike in the case of 25 mm tube diameter, where only a few droplets can be seen. The formation of big waves (large enough to lead to droplet entrainment) is confined initially to the bottom part of test section. However, droplets could be seen further up because some of these are carried away by the air stream. As the flooding air velocity is approached for a given water flow rate, larger waves are formed and some of these are taken up a short distance by the air stream. These then collapse to give rise to extensive droplet entrainment. This process of large wave generation, being carried up and breaking up, is repeated continuously,

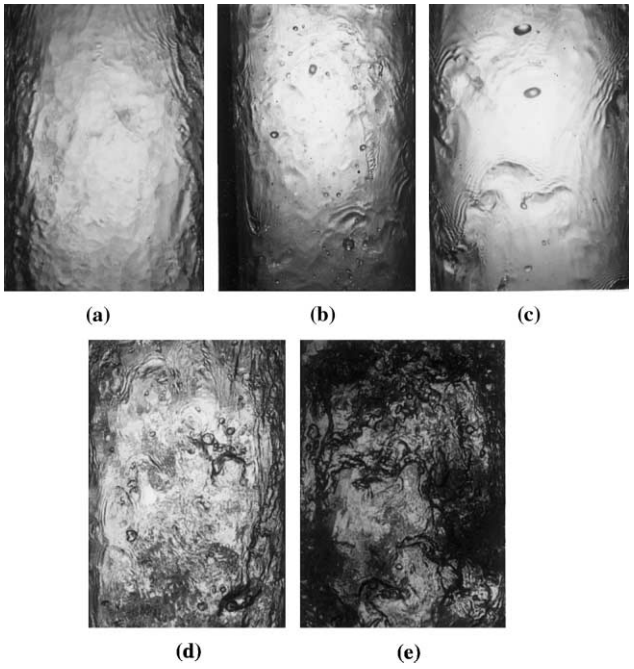

Fig. 4. Still photograph of the flow in the 67 mm diameter test section at a water flow of 0.111 kg/s and at an air flow rate of: (a) 0; (b) 0.0039; (c) 0.019; (d) 0.062; (e) 0.079 kg/s.

giving the appearance of churn-like flow of the liquid. Typically, the churning regime is confined to a small length of the tube. A photograph of this churn-like zone is shown in Fig. 4(d) which is taken at an air flow rate of 0.055 kg/s. At higher air flow rates, the churning motion becomes more violent (Fig. 4(e)) and may spread up the tube. This confined churn-like flow structure does not appear in the 25 mm diameter tube.

The pressure drop and the down flow rate of the test section measured in the 67 mm tube diameter are shown in Fig. 5 for the same water flow rate. These show that the pressure drop does not change appreciably as long as the air flow rate is insufficient to create the churn-like flow structure. Similarly, the down flow rate begins to decrease only after the formation of churn-like region; any droplets carried away by the air stream constitute a very small part of the total liquid flow rate.

Some of the still photographs taken in 99 mm diameter tube are shown in Fig. 6. Due to the large diameter of the tube, churning motion could be created only in the case of the largest possible water flow rate of 0.444 kg/s and photographs for this water flow rate are shown. It can be seen from Fig. 6(a) that the droplets are generated at fairly low air flow rates, but that large waves could be created only at much higher air flow rates. The general pattern of the flow structure is similar to that in Fig. 4 for the 67 mm diameter tube. The flow structure in the churning zone (Fig. 6(d)) at the highest air flow rate used in this test section is similar to that in Fig. 4(d) for the 67 mm diameter tube. It appears likely that if higher water/air flow rates are used, more chaotic film flow, as evident in Fig. 4(e), may also be achieved in the 99 mm diameter tube.

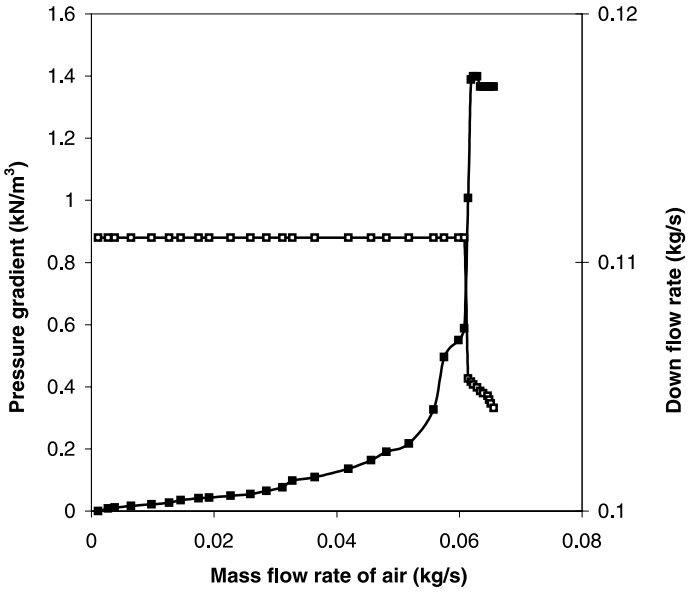

Fig. 5. Variation of the pressure gradient and the down flow rate with air flow rate at a water flow rate of 0.111 kg/s in the 67 mm diameter section.

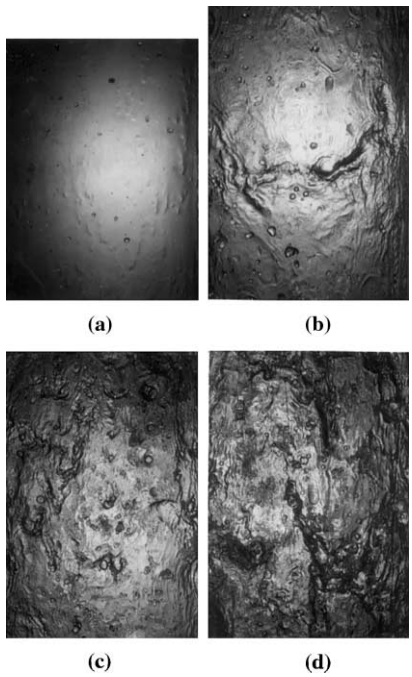

Fig. 6. Still photographs of the flow in the 99 mm diameter test section at a water flow of 0.444 kg/s and at an air flow rate of: (a) 0.005; (b) 0.044; (c) 0.0526; (d) 0.0538 kg/s.

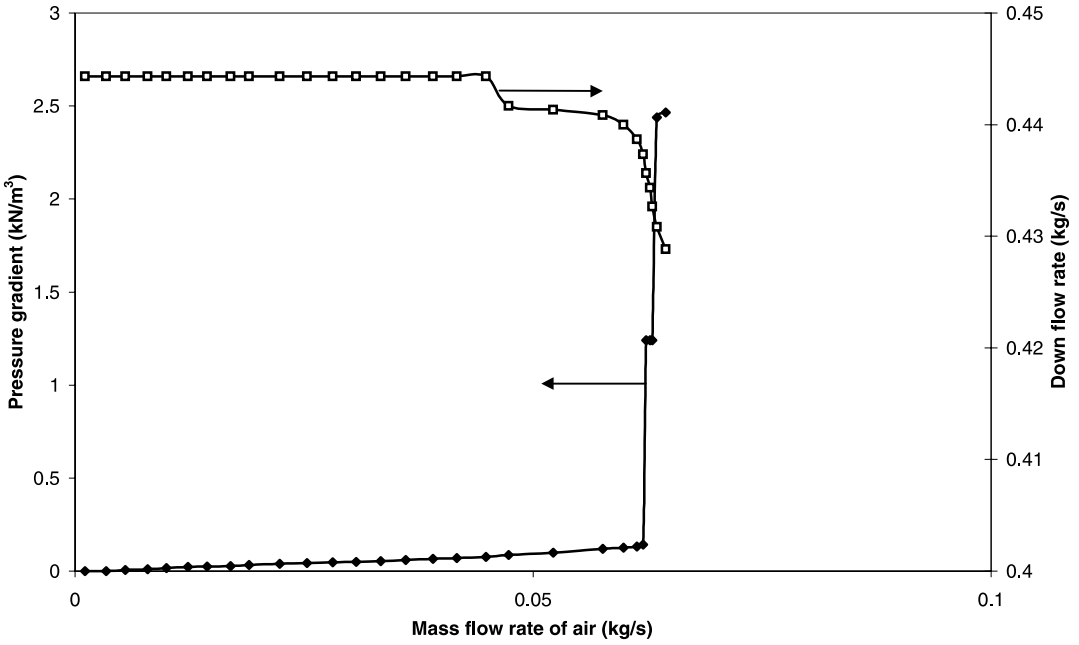

Fig. 7. Variation of the pressure gradient and the down flow rate with air flow rate at a water flow rate of 0.444 kg/s in the 99 mm diameter section.

The pressure drop in the test section and the down flow rate measured in the 99 mm diameter tube are shown in Fig. 7. Once again, it is evident that the sudden increase in the pressure gradient and a sudden decrease in the down flow rate are possible only after a churn-like motion is created in the liquid film.

3.3. Flooding mechanisms and the effect of tube diameter

The above discussion of the various events or phenomena that occur when the air flow rate is increased while maintaining the water flow rate constant leads to the possible mechanisms of flooding. Keeping in mind that flooding may be said to have occurred when liquid is found beyond the liquid inlet, *three* (and not two as is usually thought) distinct mechanisms can be readily identified. These are: (a) upward transport of large ring-type waves, (b) carryover of liquid in the form of entrained droplets by the gas stream and (c) carryover of liquid in the form of large wave in churn-like liquid flow. The conditions and the manner in which each of these occur are described below.

3.3.1. Flooding by upward transport of ring-type waves

This mechanism is found to occur only in the 25 mm diameter tube and not in the 67 and 99 mm diameter tubes. Here, at low air flow rates, the liquid film flows down essentially undisturbed by the presence of the air. At higher air flow rates, larger amplitude waves are formed near the liquid

outlet from which some droplets are sheared off. However, these droplets are deposited within a short distance from the point of inception and do not reach the top of the test section. If the air flow rate is further increased, then more droplets may be formed but before the droplet entrainment rate becomes significant enough, ring-type waves are formed on the interface around the periphery of the tube. Occasionally, some of these are taken up by the gas stream for a short distance. At still higher air flow rates, the amplitude of these ring-type waves becomes large enough to significantly restrict the cross-sectional area available for air flow. Bridging of the tube may occur in some cases. At this stage, some of these waves are swept up beyond the liquid inlet and may traverse the entire length of the test section. If the air and water flow rates are now maintained constant, then this process of large wave formation near the liquid outlet and their being swept up beyond the liquid inlet happens repeatedly and flooding occurs. There is a large amount of bubble entrainment in these large upward-moving waves. This type of flooding takes place over a small range of air flow rates and is a catastrophic process (Hewitt, 1989). The pressure gradient shows a sudden rise at the onset of flooding, and it can be a good indicator of which flooding of this type occurs.

3.3.2. Flooding by carryover of liquid in the form of entrained droplets

This mechanism is found to occur in the large (67 and 99 mm) diameter tubes at low liquid flow rates only. Here, as the gas flow rate is increased, small droplets are formed near the liquid outlet but these droplets are deposited immediately. As the gas flow rate is increased further, the droplet flux increases and the droplets can be seen at higher points in the test section. At sufficiently high gas flow rates, the droplets are carried beyond the liquid inlet and flow out of the system through the top outlet. Thus, under these conditions, there is a small but detectable flow rate of liquid from the top outlet, thus constituting flooding. At this stage, large, upward-moving waves are not seen. In some cases, large waves may be present in the bottom half of the test section but the top part has only droplets. With further increase in the gas flow rate, only the droplet flux increases, and the waves do not spread to the entire test section. The pressure drop in the test section may not show a steep rise at the onset of flooding by this mechanism. Hence using this as a criterion for flooding would be incorrect in this case.

3.3.3. Flooding by carryover of liquid in the form of large waves in churn-like flow

This type of mechanism is found to occur in the 67 mm diameter tube at sufficiently high liquid flow rates (and it is believed that, given sufficient air flow rate, it would also occur in the 99 mm diameter tube). At high liquid rates and low gas flow rates, large waves are formed near the bottom which move up for the short distance and then break up, giving rise to a number of droplets. The droplets are immediately deposited because of the low gas flow rates. Repeated occurrences of creation, upward movement and collapse of these large waves give it an appearance of churning motion. This process takes some time to establish, typically, of the order of several seconds. After this, churning motion is confined only to a small region near the liquid outlet. At this point, droplets can be seen in the top half of the test section, but no large waves are present. As the gas flow rate is further increased, this churning region becomes extended to a larger section of the tube, and some of the droplets may even reach beyond the liquid inlet. However, there is very little flux of liquid from the top outlet. Once the churning

region spreads up to the entire bottom half of the test section, the situation becomes sensitive to air flow rate. At this point, while churning motion is confined to the bottom half, large waves are lifted up periodically before they fall back into the churning zone. If the gas flow rate is further increased slightly, then some of these waves may reach beyond the liquid inlet at which point the churning motion spreads slowly to the inlet and beyond, and thus the entire test section may be under churning motion. Once this happens, liquid is seen to come out of the top outlet essentially as a wavy film. Further increase in the gas flow rate leads to an increase in the churning intensity near the inlet and a decrease near the outlet, and eventually churning motion ceases at the bottom near the outlet. This is a clear indication that in this mechanism, the flooding is independent of what happens at the liquid outlet and is determined by the redistribution of the liquid as it enters through the inlet. The pressure drop, in this case, shows a sudden rise at the onset of flooding, and therefore it can be a good indicator of when flooding of this type occurs.

The results obtained in the present study on the mechanism of flooding are partly in agreement with those obtained by other researchers in similar geometries. The first mechanism, namely, upward transport of ring-type waves, has been observed, among others, by Suzuki and Ueda (1977), McQuillan et al. (1985) and Govan et al. (1991). It is also interesting to note that the tube diameter in all these studies is fairly small (less than 32 mm). The second mechanism found in the present study, namely, carryover by droplets alone without any waves being present at the liquid inlet has not been reported by others. The third mechanism, i.e., carryover in churn-like liquid flow at the inlet has been observed indirectly by Zabaras and Dukler (1988) and Biage (1989). Zabaras and Dukler suggested that flooding occurred by flow reversals within large waves created at the inlet. Biage et al. found from their film thickness measurements that at sufficiently high air flow rates, large waves were created near the bottom in their channel of a cross-section of 0.25×0.025 m. With increasing air flow rate, these large amplitude waves spread up the tube, and flooding occurred only when large amplitude waves were created close to the inlet. This is exactly the situation recorded visually in the present experiments in which the third mechanism prevailed. Zabaras and Dukler found no upward-moving waves in their experiments while Biage et al. reported that the large waves moved up only a short distance. Recently, Watson and Hewitt (1998) conducted axial view experiments in a test section of 82 mm diameter and found that there were no ring-type waves at the flooding point. They reported that flooding was caused by an unstable churn-like flow in the liquid film.

The present experimental results from 25, 67 and 99 mm diameter tubes, taken together with the above observations from literature, clarify to a large extent the possible mechanisms by which flooding may occur. Given the liquid must be taken up beyond the liquid injection point for flooding to occur, the present study has identified three possible means of taking away excess liquid flow rate: right from the bottom in the form of coherent waves; in the form of droplets; and in the form of non-coherent waves formed close to the inlet. In the first case, and to some extent, in the second case, the flooding process is determined by what happens close to the liquid outlet while in the third case, what happens close to the inlet is of prime importance. Some of the finer details of the mechanisms still remain unknown, though, for example, how the flow split occurs close to the inlet in the third mechanism, and the process for formation of large amplitude, large wavelength waves close to flooding, and the stability of ring-type waves in different tube diameters.

4. Prediction of onset of flooding

There are a number of correlations in the literature to predict the onset of flooding, i.e., to calculate the gas flow rate at which flooding would occur for a given liquid flow rate. These correlations fall mainly into three categories:

(i) Correlations of the Wallis-type, where the flooding gas and liquid superficial velocities are correlated as (Wallis, 1961; Hewitt and Wallis, 1963)

$$\sqrt{U_G^*} + C_1\sqrt{U_L^*} = C_2, \tag{1}$$

where U_G^* and U_L^* are the dimensionless gas and liquid superficial velocities given by

$$U_G^* = U_G\sqrt{\frac{\rho_G}{gD\Delta\rho}} \quad \text{and} \quad U_L^* = U_L\sqrt{\frac{\rho_L}{gD\Delta\rho}}. \tag{2}$$

(ii) Correlations of the Kutateladze type, where the flooding gas and liquid superficial velocities are correlated as (Sun, 1979) in terms of the phase Kutateladze numbers

$$Ku_G^{*1/4} + C_3 Ku_L^{*1/4} = C_4, \tag{3}$$

where Ku_G^* and Ku_L^* are the dimensionless gas and liquid superficial velocities given by

$$Ku_G^* = U_G\left(\frac{\rho_G^2}{g\sigma\Delta\rho}\right)^{1/4} \quad \text{and} \quad Ku_L^* = U_L\left(\frac{\rho_L^2}{g\sigma\Delta\rho}\right)^{1/4}. \tag{4}$$

(iii) Correlations involving other parameters where the gas and liquid superficial velocities are correlated in terms of other parameters, for example, by Feind (1960) as

$$m\frac{Re_G}{Re_{SL}^n}\left(\frac{\rho_L}{\rho_G}\right)^{0.4}\left(\frac{\mu_G}{\mu_L}\right)^{0.75} + 1.4\times 10^4 = 1300\left(\frac{D}{2\delta}\right)^{1.2}, \tag{5}$$

where

$$\begin{aligned} &m = 92.0, \quad n = 0.33 \qquad \text{if } Re_{SL} < 1600,\\ &m = 315.4, \quad n = 0.5 \qquad \text{otherwise,} \end{aligned}$$

where Re_{SL} is based on the superficial liquid velocity and the tube diameter.

The Wallis-type correlation has the tube diameter as a parameter and the Kutateladze-type does not. This has led to some debate as to whether or not the tube diameter has an effect on flooding and attempts have been made to reconcile the two views. Richter (1981) and Jayanti et al. (1996) suggested, based on different arguments, that the Wallis-type correlation would work well in small diameter tubes and the Kutateladze-type in large diameter tubes. In order to verify this suggestion, the data obtained in the present study are compared in Figs. 8(a) and (b) with the correlations of Hewitt and Wallis (1963) and of Sun (1979). Fig. 8(a) shows the data for 25 mm diameter tube, and it can be seen that the Hewitt and Wallis (1963) correlation (with the constants C_1 and C_2 having values of 1.0 and 0.88, respectively) predicts the data better although, at high liquid flow rates, the correlation goes through a minimum that is not physically possible. The data in the 67 mm diameter tube are compared in Fig. 8(b); here the Sun (1979) correlation of the

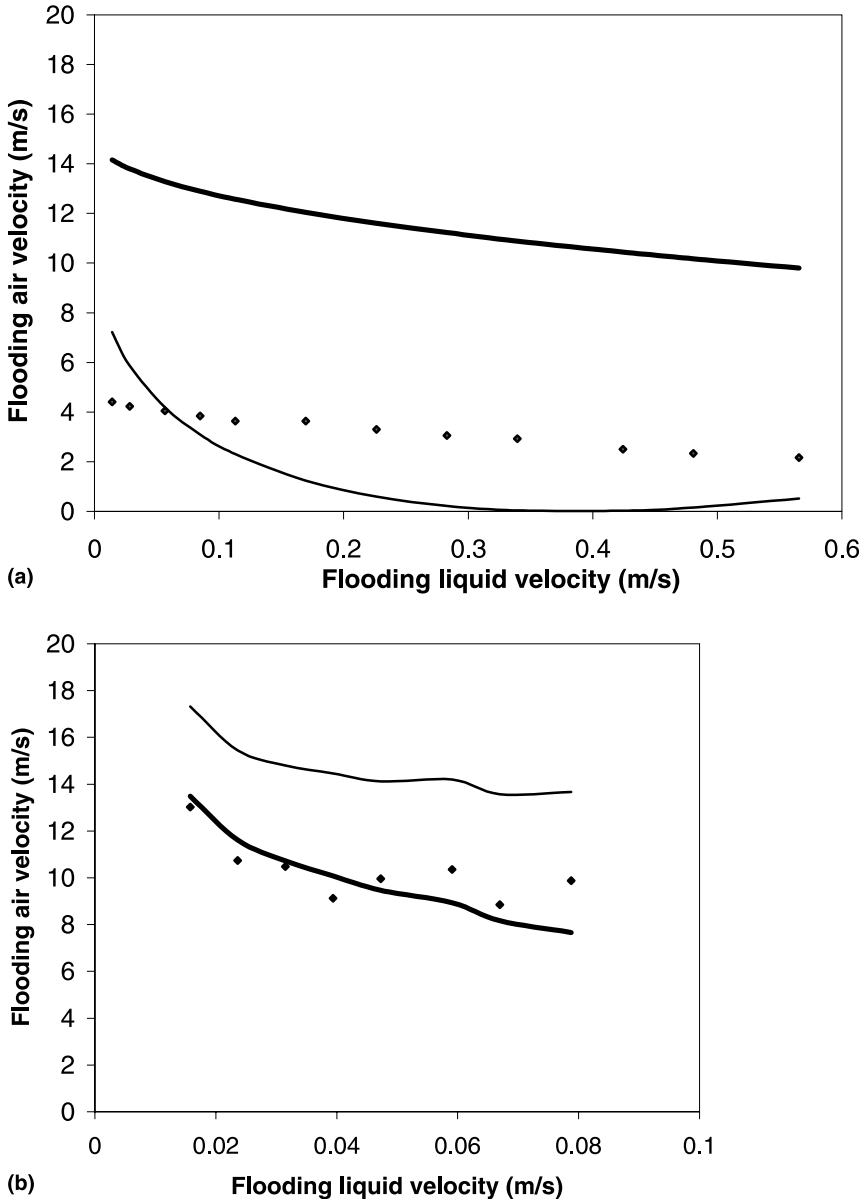

Fig. 8. (a) Comparison of the experimental data of the gas velocity at flooding with that predicted by the correlations of Hewitt and Wallis (1963) (thin line) and Sun (1979) (thick line). The symbols represent data obtained from the present experiment in the 25 mm diameter section. (b) Comparison of the experimental data of the gas velocity at flooding with that predicted by the correlations of Hewitt and Wallis (1963) (thin line) and Sun (1979) (thick line). The symbols represent data obtained from the present experiment in the 67 mm diameter section.

Kutateladze-type (with the constants C_3 and C_4 having values of 1.0 and 1.79, respectively) performs much better than that of the Hewitt and Wallis (1963) correlation, which over predicts the flooding velocities considerably.

Although the two types of correlation exhibit the expected trend with increasing tube diameter, neither of them is completely satisfactory. McQuillan et al. (1985) compared the performance of several empirical and semi-empirical correlations against a data set of 2762 data points compiled from the literature on flooding involving data obtained using a number of fluids and a large range of tube diameters and test section lengths. They concluded that among the empirical correlations, that of Alekseev et al. (1972) performed the best with a weighted error of 28%

$$Ku_G = 0.2576 Fr^{-0.22} Bo^{-0.26}, \tag{6}$$

where Ku_G is the gas phase Kutateladze number defined above, and Fr and Bo are the Froude number and the Bond number, respectively, and are defined as

$$Fr = \frac{Q_L g^{0.25} (\rho_L - \rho_G)^{0.75}}{\sigma^{0.75}}, \tag{7}$$

$$Bo = \frac{D^2 (\rho_L - \rho_G) g}{\sigma}. \tag{8}$$

McQuillan et al. (1985) proposed an improved version of the correlation to take account of viscosity of liquids

$$Ku_G = 0.268 Bo^{0.26} Fr^{-0.22} \left[1 + \frac{\mu}{\mu_L}\right]^{-0.18}$$

This correlation performed better, with the weighted error being reduced to 26%. Among the semi-empirical correlations, they found that the correlation of Bharathan et al. (1978) performed the best with a weighted error of 35%

$$\frac{2 f_w U_L^{*2}}{(1-\alpha)^2} + \frac{2 f_i U_G^{*2}}{\alpha^{2.5}} = (1-\alpha), \tag{9}$$

$$\begin{aligned} f_i &= f_w + 14.6(1-\alpha)^{1.87}, \\ f_w &= 0.005. \end{aligned} \tag{10}$$

In view of these recommendations, the data obtained in the present study in the 25 and 67 mm diameter tubes are compared with the predictions from Eqs. (6) and (9). The results are shown in Fig. 9. It can be seen that the correlation of Alekseev et al. shows excellent agreement with the data from the 25 mm diameter tube (Fig. 9(a)), but that it underpredicts the data in the 67 mm diameter tube (Fig. 9(b)). The correlation of Bharathan et al. overpredicts the data considerably in both the cases.

To summarize, the above comparison with various correlations shows that the data in the 25 mm diameter are predicted well by the correlations of Hewitt and Wallis (1963) and Alekseev et al. (1972) both of which have the tube diameter as a significant parameter. The data in the 67 mm diameter tube are predicted well by the Kutateladze-number-based correlation of Sun (1979), which overpredicted considerably the data in the smaller diameter tube. These observations lend credence to the argument that the tube diameter is an important parameter in determining the flooding velocities in small tube diameters.

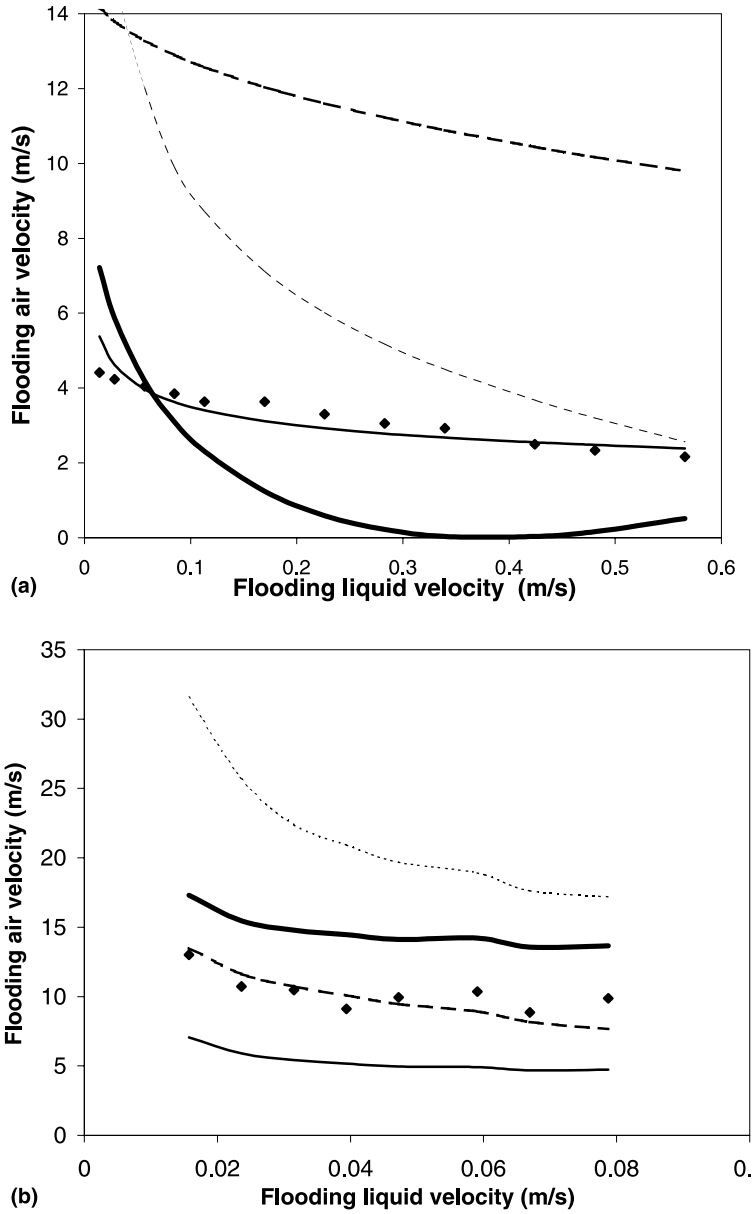

Fig. 9. (a) Comparison of the experimental data of the gas velocity at flooding with that predicted by the correlations of Alekseev et al. (1972) (thin line), Sun (1979) (dotted thick line), Hewitt and Wallis (1963) (thick line) and Bharathan et al. (1978) (dotted thin line). The symbols represent data obtained from the present experiment in the 25 mm diameter section. (b) Comparison of the experimental data of the gas velocity at flooding with that predicted by the correlations of Alekseev et al. (1972) (thin line), Sun (1979) (dotted thick line), Hewitt and Wallis (1963) (thick line) and Bharathan et al. (1978) (dotted thin line). The symbols represent data obtained from the present experiment in the 67 mm diameter section.

5. Effect of length

The effect of test section length of flooding has been investigated by a number of researchers. Hewitt et al. (1965), Suzuki and Ueda (1977) and McQuillan et al. (1985) reported that the gas velocity required for flooding increases at the same liquid flow rate as the test section length decreases. Hewitt (1977) reported no length effect when a sharp exit condition was used to remove the liquid. Zabaras and Dukler (1988), who used a porous sinter for liquid inlet, reported no length effect in their experiments in a 50.8 mm diameter tube. Recently, Jeong and No (1966) reported that the length of the test section had an effect on the flooding velocity when smooth inlet and outlet conditions were created for the liquid flow, and the test section length did not matter if a sharp exit was provided for the liquid. In the present study, the focus was not just on what air velocity was required to cause flooding but also on how the flooding was caused. To this end, experiments have been conducted in a test section length of 0.5 m (in addition to those already reported for a length of 1.8 m) specifically to study if the mechanism of flooding changes with test section length.

In the 25 mm diameter tube, the effect of changing the test section length was not remarkable in that flooding always occurred by the upward wave transport mechanism. The only change in the result between the two test section lengths was that the air flow rate required for flooding was higher in the 0.5 m long test section at the same water flow rate. The difference was more at low water flow rates.

In the case of the 67 mm diameter tube, the results for the 0.5 m long tube showed a qualitative change from those obtained in the 1.8 m long tube at the same liquid flow rates. It was found that in the 0.5 m long section, flooding did not occur for water flow rates 0.055, 0.083 and 0.111 kg/s even at the highest air flow rate. In the 1.8 m long section, this happened only at 0.0278 kg/s, and flooding occurred by the second mechanism (droplet carryover) for water flow rates of 0.055 and 0.083 kg/s and by the third mechanism (carryover due to churning motion) for higher water flow rates. In the 0.5 m long section, flooding by the second mechanism occurred at 0.139 and 0.166 kg/s and the third mechanism prevailed only at higher water flow rates. Thus, a decreased length of the test section delayed the onset of flooding by the third mechanism. At all flow rates, it was found that a higher air flow rate was required for flooding to take place in the shorter test section. This may be attributed to the wave height being less in a shorter section for the same liquid flow rate because of the shorter "fetch" or distance available for the growth of the waves.

Although a number of studies of flooding have been conducted in different tube lengths, only Jayanthi and Hewitt (1992) have proposed a correlation to take explicit account of the length of the test section. Using the data of Hewitt et al. (1965) in a tube diameter of 31.8 mm, they suggested a modification to the Hewitt and Wallis (1963) correlation to take account of the length effect:

$$\sqrt{U_{SG}^*} + m\sqrt{U_{SL}^*} = C, \tag{11}$$

where the coefficient m is the function of L/D and is given by

$$\begin{aligned} m &= 0.1928 + 0.01089\left(\frac{L}{D}\right) - 3.754 \times 10^{-5}\left(\frac{L}{D}\right)^2 \quad \text{if } L/D < 120, \\ m &= 0.96 \approx 1 \quad \text{if } L/D > 120. \end{aligned} \tag{12}$$

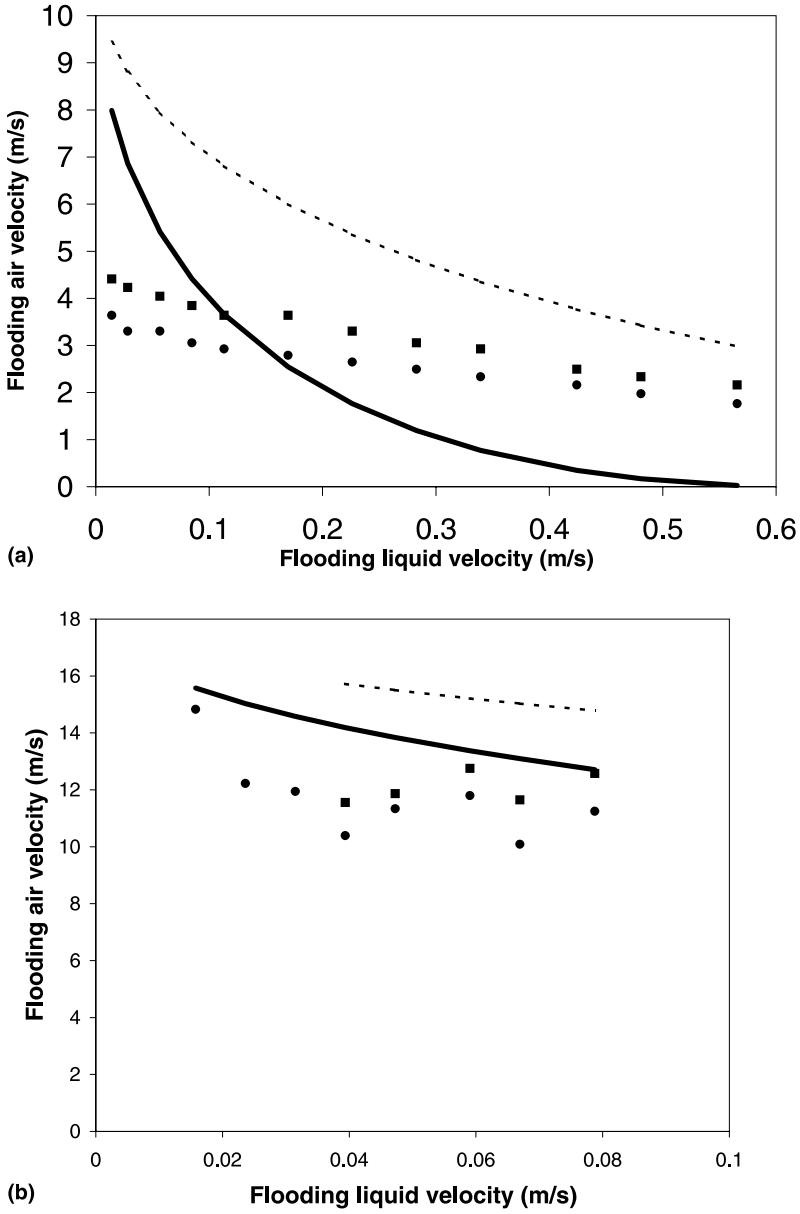

Fig. 10. (a) Comparison of the gas velocity required for flooding in the test section length of 0.5 m (squares and dotted line) and 1.8 m (diamonds and solid line). The symbols represent data obtained from the present experiment where as the curves represent the correlation of Jayanti and Hewitt (1992) for the 25 mm diameter test section. (b) Comparison of the gas velocity required for flooding in the test section length of 0.5 m (squares and dotted line) and 1.8 m (diamonds and solid line). The symbols represent data obtained from the present experiment where as the curves represent the correlation of Jayanti and Hewitt (1992) for the 67 mm diameter test section.

The above correlation has been applied to the present data from 0.5 and 1.8 m long test sections, and the results are given in Fig. 10(a) for the 25 mm diameter tube and in Fig. 10(b) for the 67 mm diameter tube. It can be seen that, although the correlation predicts the right trend, i.e., increasing gas velocity with decreasing tube length for a given liquid velocity, the predictions do not match quantitatively. The effect of the test section length on flooding therefore remains to be quantified accurately.

6. Summary and discussion

In this paper, experimental results obtained from flow visualization studies and pressure drop and down flow rate measurements in three tubes of different diameters are presented. The major phenomena which occur in countercurrent flow, as far as flooding is considered, are identified. These are the formation of large waves; the creation of droplets; the formation of ring-type waves and of upward-moving waves in the 25 mm diameter tube. In the 67 and 99 mm diameter tubes, the last two are absent. Here, a churn-like unstable liquid film flow regime occurs just prior to flooding. These phenomena provide three possible ways in which flooding may take place, namely, by upward transport of waves; by carryover of liquid in the form of droplets; and by carryover of liquid in churn-like motion. The first of these mechanisms has been found to occur only in the 25 mm diameter tube. The second one occurs in the 67 and 99 mm diameter tubes at low liquid flow rates while the third occurs at large liquid flow rates.

The simultaneous measurement of the pressure gradient and the down flow rate along with flow visualization shows that the sudden rise in pressure gradient is associated with the formation of upward transport waves, or of the churn-like motion. The generation of droplets does not cause, in itself, the steep rise in pressure gradient. Thus, the pressure gradient variation with air flow rate is a good indicator of flooding, except in the second mechanism where flooding occurs by carryover of droplets. Here, the point of flooding should be set as that flow rate at which some liquid appears above the inlet. The flooding velocities obtained in the present study of the 25 mm diameter tube are predicted well by correlations involving the tube diameter as a significant parameter (for example, those of Hewitt and Wallis, 1963; Alekseev et al., 1972) while the data in the 67 mm tube are predicted well only by the Kutateladze-type of correlation of Sun (1979), which does not involve the tube diameter as a parameter.

The effect of test section length has also been investigated by conducting flooding experiments in a test section of 0.5 m long in all the three tube diameters. It has been found that decreasing the length did not change the mechanism of flooding in the 25 mm diameter tube but did so in some cases in the 67 mm diameter tube. In all the cases, it was found that a higher gas velocity was required for flooding in the shorter test section.

Acknowledgements

The work described in the paper was carried out as part of a research project sanctioned by the Department of Science and Technology, India.

References

Alekseev, V.P., Poberezkin, A.E., Gerasimov, P.V., 1972. Determination of flooding rages in regular packings. Heat Trans. – Soviet Res. 4, 159–163.

Bankoff, S.G., Lee, S.C., 1982. A critical review of the flooding literature. US Nuclear Regulatory Commission. Report No. NUREG/CR-3060.

Bharathan, D., Wallis, G.B., Richter,H.J., 1978. Air–water countercurrent annular flow. EPRI Report No. NP-786.

Biage, M., 1989. Structure de la surface libre d'un film liquide ruisselant sur une plaque plane verticale et soumis a un contrecourant de gas: transition vers l'ecoulement cocourant ascendant. Ph.D. thesis, Institut National Polythenique de Grenoble. Grenoble, France.

Clift, R.C., Pritchard, C.L., Nedderman, R.M., 1966. The effect of viscosity on the flooding conditions in wetted wall columns. Chem. Engrg. Sci. 21, 87–95.

Dukler, A.E., Smith, L., 1982. Two-phase interactions in counter current flow: studies of the flooding mechanism. Annual Report, No. 1985–October 1987, NUREG/CR-0617, US Nuclear Regulatory Commission. Washington, DC.

Feind, F., 1960. Falling liquid films with countercurrent air flow in vertical tubes. VDI-Forschungscheft, 481, 26.

Govan, A.H., Hewitt, G.F., Richter, H.J., Scott, A., 1991. Flooding and churn flow in vertical pipes. Int. J. Multiphase Flow 17, 27–44.

Hewitt, G.F., 1982. In: Hetsroni, G. (Ed.), Handbook of Multiphase Flow Systems. McGraw-Hill, New York.

Hewitt, G.F., Wallis, G.B., 1963. Flooding and associated phenomena in falling film flow in a vertical tube. UKAEA Report, AERE R-4022.

Hewitt, G.F., Lacey, P.M.C., Nicholls, B. 1965. Transitions in film flow in a vertical tube. Symposium on Two-phase Flow, Paper B4. Exeter, England.

Hewitt, G.F., 1977. Influence of end conditions, tube inclination and physical properties on flooding in gas–liquid flows, UKAEA Report No. HTFS-RS222.

Hewitt, G.F., 1989. Countercurrent two-phase flow Invited lecture, Fourth International Topical Meeting on Nuclear Reactor Thermal Hydraulics. Karlsruhe, Germany.

Jayanti, S., Hewitt, G.F., 1992. Prediction of the slug-to-churn flow transition in vertical two-phase flow. Int. J. Multiphase Flow, 18, 847–860.

Jayanti, S., Tokarz, A., Hewitt, G.F., 1996. Theoretical investigation of the diameter effect on flooding in countercurrent flow. Int. J. Multiphase Flow 22, 307–324.

Jayanti, S., Wilkes, N.S., Clarke, D.S., Hewitt, G.F., 1990. The prediction of flow over rough surfaces and its application to the interpretation of mechanisms of horizontal annular flow. Proc. Royal Soc. Lond. A431, 71–88.

Jeong, J.H., No, H.C. Experimental study on the pipe length and pipe-end geometry on flooding. Int. J. Multiphase Flow 22, 499–514.

Mcquillan, K.W., Whalley, P.B., Hweitt, G.F., 1985. Flooding in vertical two-phase flow. Int. J. Multiphase Flow 11, 741–760.

Richter, H.J., 1981. Flooding in tubes and annuli. Int. J. Multiphase Flow 7, 647–658.

Sun, K.H., 1979. Flooding correlations for BWR bundle upper tieplates and bottom side-entry orifices. In: Veziroglu T.N. (Ed.), Proceedings of Multiphase Flow and Heat Transfer Symposium Workshop. Miami Beach, Florida, pp. 1615–1635.

Suzuki, K.H., Ueda, T., 1977. Behaviour of liquid films and flooding in countercurrent two-phase flows Part 1, Flow in circular tubes. Int. J. Multiphase Flow 3, 517–532.

Watson, M., Hewitt, G.F., 1998. Effect of diameter on flooding initiation mechanism. Third International Conference on Multiphase Flow. Lyon, France, June 8–12 1998.

Zabaras, G.J., Dukler, A.E., 1988. Countercurrent gas–liquid annular flow including the flooding state. AIChE 34, 389–396.